ARTICLE

Product Identification and Mass Spectrometric Analysis of n-Butane and i-Butane Pyrolysis at Low Pressure

Yi-jun Zhang[a,b], Wen-hao Yuan[b], Jiang-huai Cai[a], Li-dong Zhang[a], Fei Qi[a,b], Yu-yang Li[b*]

a. National Synchrotron Radiation Laboratory, University of Science and Technology of China, Hefei 230029, China

b. State Key Laboratory of Fire Science, University of Science and Technology of China, Hefei 230026, China

(Dated: Received on January 8, 2013; Accepted on January 28, 2013)

The pyrolysis of n-butane and i-butane at low pressure was investigated from 823−1823 K in an electrically heated flow reactor using synchrotron vacuum ultraviolet photoionization mass spectrometry. More than 20 species, especially several radicals and isomers, were detected and identified from the measurements of photoionization efficiency (PIE) spectra. Based on the mass spectrometric analysis, the characteristics of n-butane and i-butane pyrolysis were discussed, which provided experimental evidences for the discussion of decomposition pathways of butane isomers. It is concluded that the isomeric structures of n-butane and i-butane have strong influence on their main decomposition pathways, and lead to dramatic differences in their mass spectra and PIE spectra such as the different dominant products and isomeric structures of butene products. Furthermore, compared with n-butane, i-butane can produce strong signals of benzene at low temperature in its pyrolysis due to the enhanced formation of benzene precursors like propargyl and C4 species, which provides experimental clues to explain the higher sooting tendencies of *iso*-alkanes than n-alkanes.

Key words: n-Butane, i-Butane, Flow reactor pyrolysis, Synchrotron vacuum ultraviolet photoionization mass spectrometry, Product identification, Mass spectrometric analysis

I. INTRODUCTION

Traditional transportation fuels such as gasoline, diesel oil and kerosene are composed of many different chemical classes, especially linear alkanes and branched alkanes [1]. Understanding the combustion chemistry of alkanes not only promotes cleaner and more efficient utilization of transportation fuels, but also facilitates development of kinetic models of biofuels with long carbon chain, such as biodiesels and large alcohols. Butane isomers including n-butane and i-butane are important components of liquefied petroleum gas, and are also excellent model fuels to study the combustion behaviors of larger linear and branched alkanes. This is mainly because butane is the smallest alkane with normal and branched isomers, and exhibits the oxidation characteristics observed in larger alkanes such as cool flame, negative-temperature-coefficient (NTC) behavior and two-stage autoignition [2−6]. Meanwhile, since butane is the largest gaseous alkane at room temperature and atmospheric pressure, it can be used to control the volatility of gasoline [7].

The pyrolysis of butane is of special interest for researchers, not only due to the importance of pyrolysis reactions including thermal decomposition and combination reactions in combustion, but also because the pyrolysis of butane is broadly applied to produce ethylene and 1,3-butadiene which are important feedstocks to manufacture plastics and rubber. Many experimental studies on the pyrolysis of butane isomers have been conducted previously [8−28]. Laser diagnostic methods [18, 23, 27, 28], gas chromatography (GC) [12−17, 20−22, 24−26] or conventional mass spectrometry (MS) [11, 19] were mainly utilized to detect pyrolysis products. For example, Golden *et al.* used electron-impact ionization MS (EI-MS) to analyze the pyrolysis products of n-butane at very low pressure [19]; Goos *et al.* studied the low pressure pyrolysis of n-butane initiated by methyl radical using laser heating, and detected products by using GC combined with MS (GC-MS) [26]; Oehlschlaeger *et al.* studied the high temperature pyrolysis of n-butane and i-butane behind shock waves to explore their pressure- and temperature-dependent decomposition rate constants, and measured the concentrations of methyl radical using ultraviolet (UV) narrow-line laser absorption [27]; very recently, Sivaramakrishnan *et al.* used H-atomic resonance absorption spectroscopy (H-ARAS) to investigate the roaming radical mechanism in the shock tube pyrolysis of i-butane

*Author to whom correspondence should be addressed. E-mail: yuygli@ustc.edu.cn, Tel.: +86-551-63607923, FAX: +86-551-65141078

[28]. However, none of these work reported comprehensive identification of pyrolysis products of butane, especially radicals and isomers, due to the inherent limitations of the conventional diagnostic methods, which cannot provide sufficient validation of pyrolysis model of butane and limits the understanding of their combustion chemistry.

In this work, synchrotron vacuum ultraviolet (VUV) photoionization mass spectrometry (SVUV-PIMS) was used to study the pyrolysis of *n*-butane and *i*-butane at low pressure. The product pools including stable products, unstable radicals, and isomeric species were identified by the measurements of photoionization efficiency (PIE) spectra. Characteristics of *n*-butane and *i*-butane pyrolysis were discussed based on the mass spectrometric analysis, and provided experimental evidences for the discussion of the decomposition pathways of butane isomers.

II. EXPERIMENTS

The experimental work was performed at National Synchrotron Radiation Laboratory, USTC in Hefei, China. The experimental method has been introduced in detail elsewhere [29−31], only a brief description is given herein. Generally, the pyrolysis apparatus is composed of a pyrolysis chamber with an electrically heated flow reactor, a differentially pumped molecular-beam sampling system and a photoionization chamber with a home-made reflectron time-of-flight mass spectrometer (RTOF-MS). The gas mixture of Ar (500 standard cubic centimeters per minute (SCCM), 99.999% purity) and each butane isomer (20.83 SCCM, ≥99.0% purity) was fed into a 6.0-mm-inner-diameter alumina flow reactor with a 50-mm length heated in the furnace. The inlet mole fraction of butane is calculated to be 4%. The pressure of the pyrolysis chamber was maintained at 3 Torr during the experiment. The pyrolysis species were sampled by a quartz nozzle, and then the formed molecular beam entered the ionization chamber through a nickel skimmer and was ionized by the tunable synchrotron VUV light. The produced ions were detected by the RTOF-MS with a mass resolving power of ∼2000.

The detailed method of temperature measurement along flow reactor centerline has been introduced in our previous work [30, 32]. In brief, a tungsten-rhenium thermocouple was put close to the middle region of the heating coil to monitor the outside temperature of the flow tube. Before and after experiment, a K-type thermocouple was put inside the flow tube to measure the centerline temperature profiles with a Ar flow rate of 520.83 SCCM. Linear extrapolation was used to calibrate the experimental temperatures beyond the high temperature limit of K-type thermocouple. The thermocouple was moved along the centerline by a feedthrough outside the pyrolysis chamber to record the temperature profile which is named after its maximum value (T_{max}). Temperatures in the following discussion all refer to T_{max}.

Two experimental modes were used in this work. To identify pyrolysis species by ionization energies (IEs), PIE spectra were measured at 1623 K when almost all pyrolysis products could be observed with enough signal intensities. The identification of molecular structure was performed by comparing the measured IEs from PIE spectra with the values in Ref.[33]. To reveal the decomposition of butane isomers and formation of pyrolysis products with temperature, a series of mass spectra were recorded from 823 K to 1823 K at appropriate photon energies to ensure near-threshold photoionization of interested species and further weighted by photon fluxes for the comparison between each other.

III. RESULTS AND DISCUSSION

A. Identification of pyrolysis species

Benefitting from the advantages of synchrotron VUV photoionization and molecular-beam sampling techniques, comprehensive pyrolysis product pools of butane isomers including many stable products, radicals and isomers were identified in this work. Figure 1 demonstrates the identification of typical pyrolysis products of butane isomers from PIE spectra, two for radicals and the other two for isomers, which are directly formed from the primary decomposition of fuels. It is recognized that radicals can hardly be detected in flow reactor pyrolysis experiments at relatively high pressures (*e.g.* 1 atm) due to their short life times and negligible concentrations at elevated pressures, and therefore flow reactor pyrolysis experiments at low pressures become the suitable tool to investigate radical information in hydrocarbon pyrolysis [34]. Figure 1(a) shows the PIE spectrum of m/z=29 in the pyrolysis of *n*-butane. An onset at 8.24 eV can be observed from the figure and indicates the existence of ethyl radical (C_2H_5, IE=8.26 eV [33]). Similarly, allyl radical (C_3H_5, IE=8.18 eV [33]) is also detected in the pyrolysis of *i*-butane isomers as shown in Fig.1(c).

Figure 1 also shows the PIE spectra of m/z=56 (C_4H_8) in the pyrolysis of butane isomers. In Fig.1(b), a clear onset around 9.10 eV reveals the formation of 2-butene (IE=9.12 eV [33]) in the pyrolysis of *n*-butane. To assist the identification of higher IE C_4H_8 species, the photoionization cross section (PICS) profile of 2-butene [35] is plotted in the figure. Then a higher onset around 9.55 eV appears, corresponding to the literature IE of 1-butene [33]. Both isomers have comparable signals as observed from the PIE spectrum. From the PIE spectrum of m/z=56 in the pyrolysis of *i*-butane (Fig.1(d)), *i*-butene (IE=9.22 eV [33]) can be detected with measured IE at 9.19 eV. Its PICS profile [36] is also used to reveal the onset of 1-butene at higher photon energy. The onset of 1-butene is so obscure that

DOI:10.1063/1674-0068/26/02/151-156

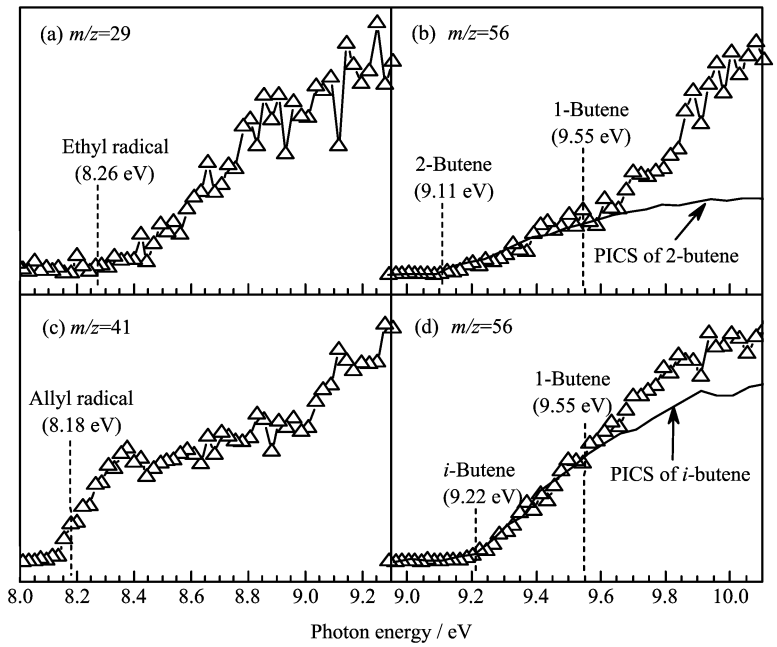

FIG. 1 PIE spectra of m/z=29 (a) and 56 (b) in *n*-butane pyrolysis and m/z=41 (c) and 56 (d) in *i*-butane pyrolysis at 1623 K. Identified species and their literature IEs are labeled at corresponding photon energies. To guide the eyes, photoionization cross section profiles of 2-butene [35] and *i*-butene [36] are drawn in (b) and (d).

one can hardly observe it without the assistance of *i*-butene's PICS profile, which indicates the dominance of *i*-butene in C_4H_8 products of *i*-butane pyrolysis. The different isomeric structures and dominance of C_4H_8 products in the pyrolysis of *n*-butane and *i*-butane are definitely related to the different molecular structures of fuels, which will be discussed in detail in the following section.

Based on the measurements of PIE spectra, more than 20 species were detected in this work. Their molecular weights, formula, names, literature IEs and measured IEs are listed in Table I. It can be seen that some radicals including CH_3, C_2H_5, C_3H_3 and C_3H_5 were detected in the pyrolysis of both *n*-butane and *i*-butane. Benefiting from the measurements of IEs, isomers of C_3H_4 and C_4H_8 were also distinguished. Due to simple molecular structures of fuels, the pyrolysis product pools of *n*-butane and *i*-butane are almost identical, except the butene isomers whose formation is directly related to the molecular structures of butane isomers.

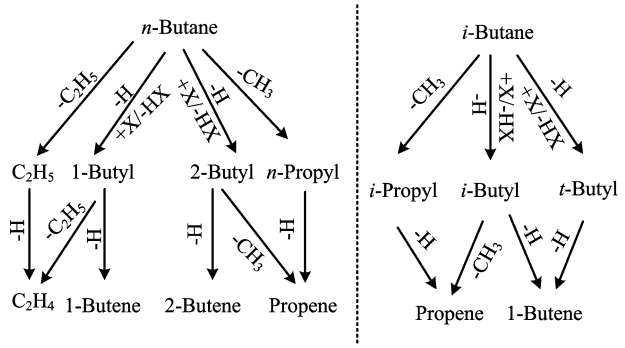

FIG. 2 Decomposition pathways of *n*-butane and *i*-butane discussed in this work. X and HX represent radicals (H, CH_3, *etc.*) and H-abstraction products by X radical attack, respectively.

B. Mass spectrometric analysis

Though the product pools in the pyrolysis of *n*-butane and *i*-butane are very similar, there are still a lot of different characteristics between them due to the different molecular structures and decomposition pathways of *n*-butane and *i*-butane (shown in Fig.2). Based on the discussion in our previous work [37, 38], it is concluded that the photon-flux-weighted ion intensity of a species in a mass spectrum is approximately proportional to its mole fraction. Therefore further insight into the pyrolysis chemistry can be obtained either from analysis of mass spectra measured at different temperatures for the same fuel or by comparing mass spectra of different fuels at similar conditions.

1. Pyrolysis of *n*-butane

Figure 3 shows the mass spectra at different temperatures in the pyrolysis of *n*-butane. All reported mass spectra in this work were measured at the photon energy of 11.0 eV to simultaneously exhibit most products (especially ethylene) and limit photofragmentation

DOI:10.1063/1674-0068/26/02/151-156

TABLE I List of species detected in the pyrolysis of butane isomers.

m/z	Species	IE[a]/eV		
		Ref.[33]	*n*-Butane	*i*-Butane
2	Hydrogen	15.43	15.45	15.42
15	Methyl radical	9.84	9.80	9.79
16	Methane	12.61	12.60	12.65
26	Acetylene	11.40	11.35	11.34
28	Ethylene	10.51	10.43	10.45
29	Ethyl radical	8.26	8.24	8.32
30	Ethane	11.52	11.55	11.53
39	Propargyl radical	8.67	8.70	8.65
40	Propyne	10.36	10.38	10.33
	Allene	9.69	9.78	9.77
41	Allyl radical	8.18	8.16	8.13
42	Propylene	9.73	9.72	9.74
50	Diacetylene	10.17	10.12	10.10
52	Vinylacetylene	9.58	9.56	9.56
54	1,3-Butadiene	9.07	9.08	9.09
56	2-Butene	9.11	9.12	–[b]
	i-Butene	9.22	–[b]	9.19
	1-Butene	9.55	9.59	9.55
58	*n*-Butane	10.53	10.50	–[b]
	i-Butane	10.68	–[b]	10.65
78	Benzene	9.24	[c]	9.26

[a] The uncertainties of measured IE are ±0.05 eV for species with strong signal/noise (S/N) ratio or ±0.10 eV for species with weak S/N ratio;
[b] The symbol "–" represents that the corresponding species was not formed at all temperautres in this work;
[c] Not formed at the temperature of PIE spectra measurements (1623 K).

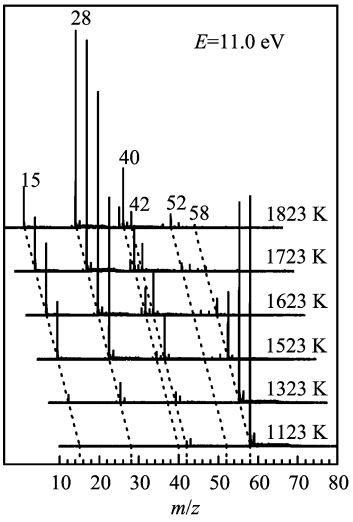

FIG. 3 Stack plots of photoionization mass spectra at different temperatures in the pyrolysis of *n*-butane. The scales of all mass spectra are identical.

of fuels. As seen from Fig.3, the decay of *n*-butane and the rise of products are unambiguously demonstrated. Methyl, ethylene and propene have strong signals among all products at both low and high temperatures, while the signals of C_3H_4 isomers become comparable at very high temperatures. C4 unsaturated products including C_4H_8, C_4H_6, C_4H_4, and C_4H_2 only have weak signals, which indicates that only a minor part of *n*-butane decomposes along sequential H-loss pathways to form C4 products in pyrolysis.

From Fig.3, it is observed that *n*-butane is almost undecomposed at 1123 K. The small peak at m/z=43 belongs to the C_3H_7 fragment of *n*-butane. At early decomposition temperatures like 1323 and 1523 K, methyl, ethylene, and propene are major observed products. Here the whole temperature region of fuel decomposition is divided into two stages, that is, the early decomposition stage for the first half region and the late decomposition stage for the last half. It is known that unimolecular dissociation of fuel controls the fuel decomposition and product formation at the early decomposition stage when radicals are in low concentration levels [32, 34]. Based on the bond dissociation energies (BDEs) of *n*-butane [39], the weakest bond in *n*-butane is the C2−C3 bond with the BDE of 86.8 kcal/mol, which is 2.1 kcal/mol lower than other two C−C bonds and at least 11.5 kcal/mol lower than the C−H bonds. Therefore the cleavage of C2−C3 bond to produce two ethyl radicals should be the most effective unimolecular decomposition pathway of *n*-butane at low temperature, while the cleavage of C1−C2 and C3−C4 bonds to produce methyl and *n*-propyl radicals is the second important one. Both ethyl and *n*-propyl radicals can suffer rapid β-C−H scission reactions to produce ethylene and propene, respectively. *n*-Propyl can also decompose via β-C−C scission to methyl and ethylene. From Fig.3, ethylene is observed as the most abundant product, while methyl and propene cannot compete with it though they also have strong signals. Therefore the experimental observations provide solid evidences for above discussion.

At the late decomposition stage, the H-abstraction reactions of fuel also have significant contributions to fuel consumption due to the accumulated concentration of radicals [32, 34]. The β-C−H scission of 1-butyl ($CH_3CH_2CH_2C^*H_2$) and 2-butyl ($CH_3CH_2C^*HCH_3$) can produce 1-butene and 2-butene, which agrees with the isomeric identification from the PIE spectrum. However, because BDEs of β-C−H bonds are at least 11 kcal/mol higher than those of β-C−C bonds in both 1-butyl and 2-butyl molecules [39], the two H-abstraction products of *n*-butane are most likely decomposed via β-C−C scission reactions to produce ethyl+ethylene and methyl+propene, respectively, rather than to decay via β-C−H scission reactions. This interprets the low signals of C4 unsaturated products in

DOI:10.1063/1674-0068/26/02/151-156

the pyrolysis of *n*-butane as observed from Fig.3.

C. Pyrolysis of *i*-butane

Figure 4 shows the mass spectra at different temperatures measured in the pyrolysis of *i*-butane. Similarly to Fig.3, the fuel decomposition and product formation with increasing temperature can be clearly observed from Fig.4. Different from the pyrolysis of *n*-butane, the pyrolysis of *i*-butane has more complex mass spectra, which leads to more products with strong signals such as methyl, ethylene, propargyl, C_3H_4 isomers, propene, vinylacetylene, and C_4H_8 isomers. In particular, C4 unsaturated products can be readily observed from the mass spectra, which indicates that *i*-butane is easier to decompose through C4 channels in pyrolysis.

As observed from Fig.4, *i*-butane remains undecomposed at 1123 K. The peak at m/z=42 can be interpreted as the C_3H_6 fragment of *i*-butane with the appearance potential of ∼10.90 eV [33, 35]. It is observed that *i*-butane has a similar initial decomposition temperature to *n*-butane. At the beginning of *i*-butane decomposition (*e.g.* 1323 K), product signals can only be unambiguously observed at m/z=15, 42, and 56, corresponding to methyl, propene and *i*-butene. The strongest peak belongs to propene even after it is subtracted by the C_3H_6 fragment signal of *i*-butane. Based on the BDEs of *i*-butane [39], the weakest bonds are three C−C bonds (88.2 kcal/mol), which are 7.5 kcal/mol lower than the C2−H bond and 12.0 kcal/mol lower than the C1−H bonds. Therefore the cleavage of C−C bonds to produce methyl and *i*-propyl radicals is the dominant unimolecular decomposition pathway of *i*-butane, and controls the consumption of *i*-butane at the beginning of its decomposition. Because the unpaired electron located at the middle carbon atom of *i*-propyl, *β*-C−H scission is the most effective and rapid consumption pathway of *i*-propyl, leading to the strong signals of propene. Furthermore, the similar dominant decomposition pathways of butane isomers, *i.e.* the cleavage of C−C bonds, should be the main reason for their similarly initial decomposition temperatures.

i-Butane can also suffer H-abstraction or unimolecular decomposition reactions to form *i*-butyl ($(CH_3)_2CHC^*H_2$) and *t*-butyl ($(CH_3)_3C^*$) radicals. Similarly to the situation in the pyrolysis of *n*-butane, the importance of these channels will be enhanced at the late decomposition stage of *i*-butane pyrolysis. Both *i*-butyl and *t*-butyl can readily suffer *β*-C−H scission reactions to produce *i*-butene, which interprets the early formation of *i*-butene and its dominance in C_4H_8 isomers. Furthermore, similarly to 1-butyl and 2-butyl, *i*-butyl is more easily to decay via *β*-C−C scission and becomes the second important precursor of propene. The decomposition of propene and *i*-butene is the main source of smaller products in the pyrolysis of *i*-butane.

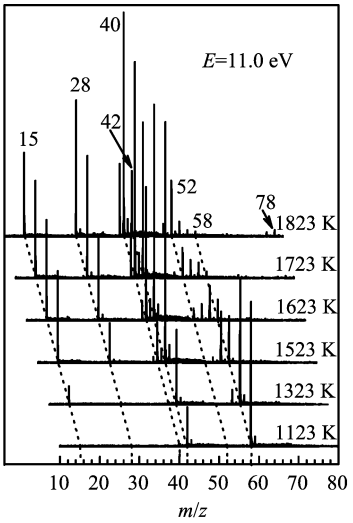

FIG. 4 Stack plots of photoionization mass spectra at different temperatures in the pyrolysis of *i*-butane. The scales of all mass spectra are identical.

It is notable that benzene was clearly detected at the late decomposition stage of *i*-butane, while only very weak signals of benzene were observed in the pyrolysis of *n*-butane. Besides, *i*-butane also produces benzene at lower temperature than *n*-butane, as seen from Table I. It is broadly recognized that the self-combination of propargyl radical and combination of C4 radicals with acetylene are two most significant formation pathways of benzene in combustion of small hydrocarbons [40]. In the pyrolysis of *i*-butane, the signals of both propargyl and C4 products are much stronger than those in the pyrolysis of *n*-butane, which results in the different behaviors of butane isomers in benzene formation. Since benzene is the precursor of PAHs and soot in combustion of small hydrocarbons, the enhanced formation of benzene in the pyrolysis of *i*-butane will provide experimental clues to explain the strong sooting tendencies of iso-alkanes compared with *n*-alkanes [41].

IV. CONCLUSION

Low pressure pyrolysis of *n*-butane and *i*-butane from 823−1823 K in a flow reactor has been studied using SVUV-PIMS. More than 20 species including several radicals and isomers were unambiguously identified from the measurements of PIE spectra. The product pools of *n*-butane and *i*-butane pyrolysis are almost identical, except for the butene isomers. Based on the mass spectrometric analysis, the characteristics of *n*-butane and *i*-butane pyrolysis were discussed. The most abundant products in the pyrolysis of *n*-butane and *i*-butane are ethylene and propene, respectively, indicating that the cleavage of C−C bonds is the dominant unimolecular decomposition pathways of butane isomers. The decomposition of *i*-butane can also lead to strong

DOI:10.1063/1674-0068/26/02/151-156

signals of *i*-butene due to its branched structure, while the formation of 1-butene and 2-butene in the pyrolysis of *n*-butane is suppressed. Furthermore, *i*-butane can produce more abundant benzene than *n*-butane due to the enhanced formation of propargyl and C4 species, which may interpret the higher sooting tendencies of iso-alkanes than *n*-alkanes.

V. ACKNOWLEDGEMENTS

This work is supported by the National Natural Science Foundation of China (No.51106146, No.51036007, No.U1232127), the China Postdoctoral Science Foundation (No.20100480047 and No.201104326), the Chinese Universities Scientific Fund (No.WK2310000010), the Anhui Science & Technology Department (No.11040606Q49), and the Chinese Academy of Sciences.

[1] M. Grayson, *Encyclopedia of Chemical Technology*, 3rd Edn., New York: John Wiley & Sons (1978).
[2] F. Battin-Leclerc, O. Herbinet, P. A. Glaude, R. Fournet, Z. Zhou, L. Deng, H. Guo, M. Xie, and F. Qi, Angew. Chem. Int. Edit. **49**, 3169 (2010).
[3] F. Battin-Leclerc, O. Herbinet, P. A. Glaude, R. Fournet, Z. Zhou, L. Deng, H. Guo, M. Xie, and F. Qi, Proc. Combust. Inst. **33**, 325 (2011).
[4] O. Herbinet, F. Battin-Leclerc, S. Bax, H. Le Gall, P. A. Glaude, R. Fournet, Z. Y. Zhou, L. L. Deng, H. J. Guo, M. F. Xie, and F. Qi, Phys. Chem. Chem. Phys. **13**, 296 (2011).
[5] M. Cord, B. Sirjean, R. Fournet, A. Tomlin, M. Ruiz-Lopez, and F. Battin-Leclerc, J. Phys. Chem. A **116**, 6142 (2012).
[6] F. Buda, R. Bounaceur, V. Warth, P. A. Glaude, R. Fournet, and F. Battin-Leclerc, Combust. Flame **142**, 170 (2005).
[7] N. M. Marinov, W. J. Pitz, C. K. Westbrook, A. M. Vincitore, M. J. Castaldi, S. M. Senkan, and C. F. Melius, Combust. Flame **114**, 192 (1998).
[8] C. D. Hurd and L. U. Spence, J. Am. Chem. Soc. **51**, 3353 (1929).
[9] G. Egloff, C. L. Thomas, and C. B. Linn, Ind. Eng. Chem. **28**, 1283 (1936).
[10] L. F. Marek and M. Neuaus, Ind. Eng. Chem. **25**, 516 (1933).
[11] A. J. B. Robertson, Proc. R. Soc. Lond., Ser. A, Math. Phys. Sci. **199**, 394 (1949).
[12] H. J. Hepp and F. E. Frey, Ind. Eng. Chem. **45**, 410 (1953).
[13] J. H. Purnell and C. P. Quinn, Nature **189**, 656 (1961).
[14] S. Sandler and Y. H. Chung, Ind. Eng. Chem. **53**, 391 (1961).
[15] C. T. Brooks, Trans. Faraday Soc. **62**, 935 (1966).
[16] R. S. Konar, R. M. Marshall, and J. H. Purnell, Trans. Faraday Soc. **64**, 405 (1968).
[17] J. E. Blakemor, J. R. Barker, and W. H. Corcoran, Ind. Eng. Chem. Fundam. **12**, 147 (1973).
[18] S. L. K. Wittig, W. A. Medwid, and T. W. Lester, Bull. Am. Phys. Soc. **19**, 1148 (1974).
[19] D. M. Golden, Z. B. Alfassi, and P. C. Beadle, Int. J. Chem. Kinet. **6**, 359 (1974).
[20] D. R. Powers and W. H. Corcoran, Ind. Eng. Chem. Fundam. **13**, 351 (1974).
[21] G. L. Pratt and D. Rogers, J. Chem. Soc., Faraday Trans. 1 **75**, 2688 (1979).
[22] G. L. Pratt and D. Rogers, J. Chem. Soc., Faraday Trans. 1 **76**, 1694 (1980).
[23] T. Koike and K. Morinaga, Bull. Chem. Soc. Jpn. **54**, 2439 (1981).
[24] L. S. Kershenbaum and P. W. Leaney, Ind. Eng. Chem. Proc. Des. Dev. **25**, 786 (1986).
[25] A. N. Rumyantsev and E. Y. Oganesova, Chem. Technol. Fuels Oils **23**, 35 (1987).
[26] E. Goos, H. Hippler, K. Hoyermann, and B. Jurges, Phys. Chem. Chem. Phys. **2**, 5127 (2000).
[27] M. A. Oehlschlaeger, D. F. Davidson, and R. K. Hanson, J. Phys. Chem. A **108**, 4247 (2004).
[28] R. Sivaramakrishnan, J. V. Michael, L. B. Harding, and S. J. Klippenstein, J. Phys. Chem. A **116**, 5981 (2012).
[29] Y. Y. Li and F. Qi, Acc. Chem. Res. **43**, 68 (2010).
[30] Y. J. Zhang, J. H. Cai, L. Zhao, J. Z. Yang, H. F. Jin, Z. J. Cheng, Y. Y. Li, L. D. Zhang, and F. Qi, Combust. Flame **159**, 905 (2012).
[31] F. Qi, Proc. Combust. Inst. **34**, 33 (2013).
[32] Y. Y. Li, L. D. Zhang, Z. D. Wang, L. L. Ye, J. H. Cai, Z. J. Cheng, and F. Qi, Proc. Combust. Inst. **34**, 1739 (2013).
[33] P. J. Linstrom and W. G. Mallard, *NIST Chemistry Webbook, National Institute of Standard and Technology*, Number 69, Gaithersburg, MD, (2011), http://webbook.nist.gov.
[34] J. H. Cai, L. D. Zhang, F. Zhang, Z. D. Wang, Z. J. Cheng, W. H. Yuan, and F. Qi, Energy Fuels **26**, 5550 (2012).
[35] B. Yang, J. Wang, T. A. Cool, N. Hansen, S. Skeen, and D. L. Osborn, Int. J. Mass spectrom. **309**, 118 (2012).
[36] J. Wang, B. Yang, T. A. Cool, N. Hansen, and T. Kasper, Int. J. Mass spectrom. **269**, 210 (2008).
[37] Y. Y. Li, L. D. Zhang, Z. Y. Tian, T. Yuan, J. Wang, B. Yang, and F. Qi, Energy Fuels **23**, 1473 (2009).
[38] Y. Y. Li, L. D. Zhang, T. Yuan, K. W. Zhang, J. Z. Yang, B. Yang, F. Qi, and C. K. Law, Combust. Flame **157**, 143 (2010).
[39] Y. R. Luo, *Comprehensive Handbook of Chemical Bond Energies*, Boca Raton, FL: CRC Press, (2007).
[40] C. S. McEnally, L. D. Pfefferle, B. Atakan, and K. Kohse-Hoinghaus, Prog. Energy Combust. Sci. **32**, 247 (2006).
[41] S. P. Crossley, W. E. Alvarez, and D. E. Resasco, Energy Fuels **22**, 2455 (2008).

DOI:10.1063/1674-0068/26/02/151-156